Egypt. J. Chem. **Vol. 66,** No. 8 pp. 129 - 139 (2023)

Egyptian Journal of Chemistry

http://ejchem.journals.ekb.eg/

Synthesis and antibacterial activity of chitosan nanoparticles from black tiger shrimp shells (*Penaeus monodon*)

Suriati Eka Putri[a,b], Ahyar Ahmad[c,d,*], Indah Raya[c], Rachmat Triandi Tjahjanto[e], Rizal Irfandi[f]

[a]*Doctoral Program, Department of Chemistry, Faculty of Mathematics and Natural Sciences, Hasanuddin University, Jalan Perintis Kemerdekaan Km. 20, Makassar, 90245, Indonesia*

[b]*Department of Chemistry, Faculty of Mathematics and Natural Science, Universitas Negeri Makassar, Makassar, Jalan Daeng Tata Raya Makassar, 90244, Indonesia*

[c]*Department of Chemistry, Faculty of Mathematics and Natural Science, Hasanuddin University, Jalan Perintis Kemerdekaan Km. 20, Makassar, 90245, Indonesia*

[d]*Research and Development Centre for Biopolymers and Bioproducts, LPPM, Universitas Hasanuddin, Makassar, 90245, Indonesia.*

[e]*Department of Chemistry, Faculty of Mathematics and Natural Science, Brawijaya University, Jalan Veteran Malang, 65145, Indonesia*

[f]*Department of Biology, Faculty of Teacher Training and Education, Universitas Puangrimaggalatung, Jalan Sultan Hasanuddin, Madukkeleng, Sengkang, 90915, Indonesia*

Abstract

Chitosan nanoparticles (CS-NPs) are potential materials for antibacterial application. This study was focused on synthesized CS-NPs from wasted black tiger shrimp shells (*Penaeus monodon*) and their antibacterial activity. The CS-NPs were synthesized using the ionic gelation method at a variated initial concentration of chitosan (CS). The characterization of CS-NPs includes functional group analysis using Fourier Transform Infra-Red (FTIR), particle size using Particle Size Analyzer (PSA), and surface morphology analysis using Scanning Electron Microscope (SEM). The results show that the degree of deacetylation (DD) of CS-NPs is more than 90%, with the average particle size of CS-NPs being 92.89 nm to 407 nm (which increased with an increasing initial concentration of CS) which is supported from the occurrence of agglomeration (the results of SEM analysis). Antibacterial activity test showed that CS-NPs were more active in inhibiting Gram-positive (*S. aureus*) bacteria than Gram-negative (*E. coli*). Therefore, the wasted black tiger shrimp shells are highly suggested as CS-NPs raw materials for bio-application.

Keywords: chitosan nanoparticles, shrimp shells, antibacterial

1. Introduction

In recent years, green chemistry has been very important and has received a lot of attention, due to it is more environmentally friendly, more efficient and sustainable [1],[2]. CS is one type of biopolymer, which is obtained from strong base deacetylation of chitin, a linear biopolymer formed by N-acetyl-D-glucosamine units linked by β (1,4) glycosidic bonds. CS has biocompatibility, biodegradability, and non-toxic properties that can be applied in several aspects of life and have been widely studied. CS applications are currently being developed, such as in the field of wastewater remediation in the environment [3], preservative supplement [4], antioxidant [5], antibacterial [6], anti-cancer [7], antidiabetic [8], and food processing [9].

In this study, CS will be used as an antibacterial. Antibacterial is divided into bacteriostatic (suppressing bacterial growth), and bactericidal, (killing bacteria) [10]. Bacteria that cause infection

*Corresponding author e-mail: ahyarahmad@gmail.com.; (Ahyar Ahmad).
EJCHEM use only: Received date 03 July 2022; revised date 06 September 2022; accepted date 12 December 2022
DOI: 10.21608/ejchem.2022.148340.6417

and disease are commonly found in our environment, including *S. aureus* and *E. coli* which are Gram-positive and Gram-negative bacteria. The growth of these bacteria will cause several diseases, such as pneumonia, wounds, endocarditis, and digestive infections. Thus, the growth of these bacteria needs to be inhibited with antibacterial [11]. Antibacterial is a substance that can inhibit the growth of bacteria and kill pathogenic bacteria [12].

CS has been shown to be effective against Gram-positive and Gram-negative bacteria because of its properties. The main mechanism of antibacterial activity involves interactions between the functional group of CS with the bacterial cell wall, cell membrane and cytoplasmic constituents via electrostatic interactions [13]. Moon et al. [14] report that CS solution is active in inhibiting bacteria. The same results were also reported by Kusnadi et al. [15] that the activity of CS inhibiting S. aureus and E. coli bacteria increased with increasing DD. However, CS was used at a fairly high concentration in these studies. Thus, currently, CS is modified to CS-NPs, the smaller size of NPs has manifested a significant change in its physical properties to its original counterpart. CS-NPs share features of CS and valuable assets of NPs, such as small size, increased surface area, and quantum size effects [16]. Kritchenkov et al. [17] reported that CS-NPs obtained by ionic gelation demonstrated a maximum antibacterial activity against *S. aureus* and *E. coli* than CS. In the same results reported by Mubarakali et al. [18], CS-NPs showed anti bactericidal activity at the lower minimum inhibitory concentration.

In general, the CS-NPs produced are synthesized from commercial CS. In contrast, chitin can be found in the exoskeleton of crustaceans and mollusca in the cuticle of insects [19], which is relatively abundant. Some crustacean wastes that have been utilized in the process of synthesizing CS-NPs, such as crab shell waste [20], white shrimp shell waste [21], deep-sea mud shrimp [22], and lobster [23]. However, the CS-NPs produced had a DD below 90%, so in this study, we attempt to find alternative crustacean waste with a reasonably high chitin content, namely from black tiger shrimp shells waste containing 20-30% chitin [24].

The use of black tiger shrimp shells as the raw material for CS synthesis has been carried out previously, producing CS with very high DD up to 99% [25]. Nevertheless, as the best we know, this crustacean waste has never been used to synthesise CS-NPs. In this study, we will examine the synthesis of CS-NPs from black tiger shrimp shells waste using the ionic gelation method and its application as antibacterial activity.

2. Experimental

2.1 Sample Preparation

The black tiger shrimp shells were obtained from Makassar, South Sulawesi, Indonesia, as much as 2 kg of shrimp shell waste was washed with water until the attached dirt was removed. Then it was dried, mashed, and sieved through a 50-mesh or 297 microns sieved, for more detail of sample preparation of CS from black tiger shrimp shown in Fig. 1.

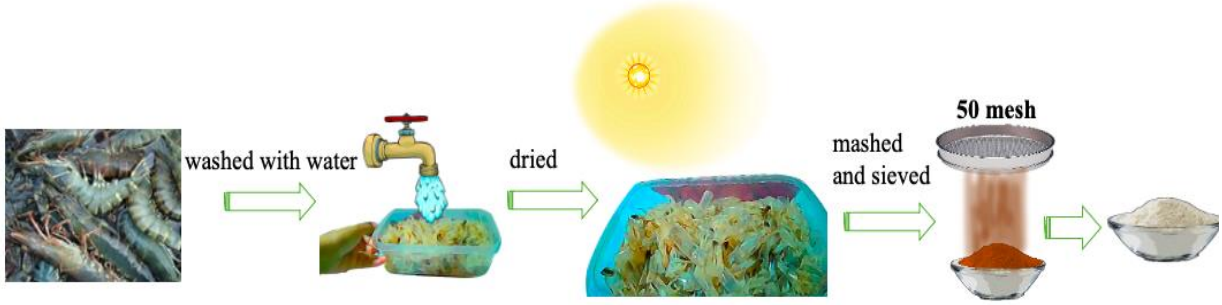

Fig. 1. Schematic illustration of sample preparation of CS from black tiger shrimp

2.2 Extraction of CS

Extraction of CS from black tiger shrimp shells waste was carried out in three steps, consisting of demineralization, deproteination, and deacetylation. The demineralization step was carried out using 1 M HCl at 90 ℃ for 3 hours. After that, it was filtered and washed with distilled water until the pH was neutral. Qualitative tests were performed with $AgNO_3$ until no white precipitate was formed, indicating that the Cl^- ions contained had vanished. Then the residue was dried at 60 ℃.

The deproteination step was carried out using NaOH 4% at 65 ℃ for 2 hours, then washed with distilled water until the pH was neutral. A qualitative test was performed with the addition of acetic acid until a precipitate was not formed. Then the residue was dried at 60 ℃. The obtained chitin was further identified using FTIR.

The deacetylation step was carried out using NaOH 50%, refluxed at 90 ℃ for 8 hours then filtered, and washed using distilled water until the pH was neutral. Furthermore, the residue was dried at a temperature of 60 ℃ until dry [18], the detail of extraction CS from black tiger shrimp shells waste is shown in Fig. 2.

The CS obtained was calculated the DD using the quantitative infrared spectrophotometric method, by calculating the % transmittance or absorbance. Calculation of DD on chitin, CS, and CS-NPs by comparing absorbance at wave number for amide group -NH (1650-1500) cm^{-1} (A 1655) with absorbance at wave number for primary amine group (3500-3200) cm^{-1} (A 3450), with an absorbance value of 1.33, based on eq. (1).

$$\%DD = 100 - \left(\frac{A_{1655}}{A_{3450}} \times 100\right) / 1.33 \quad (1)$$

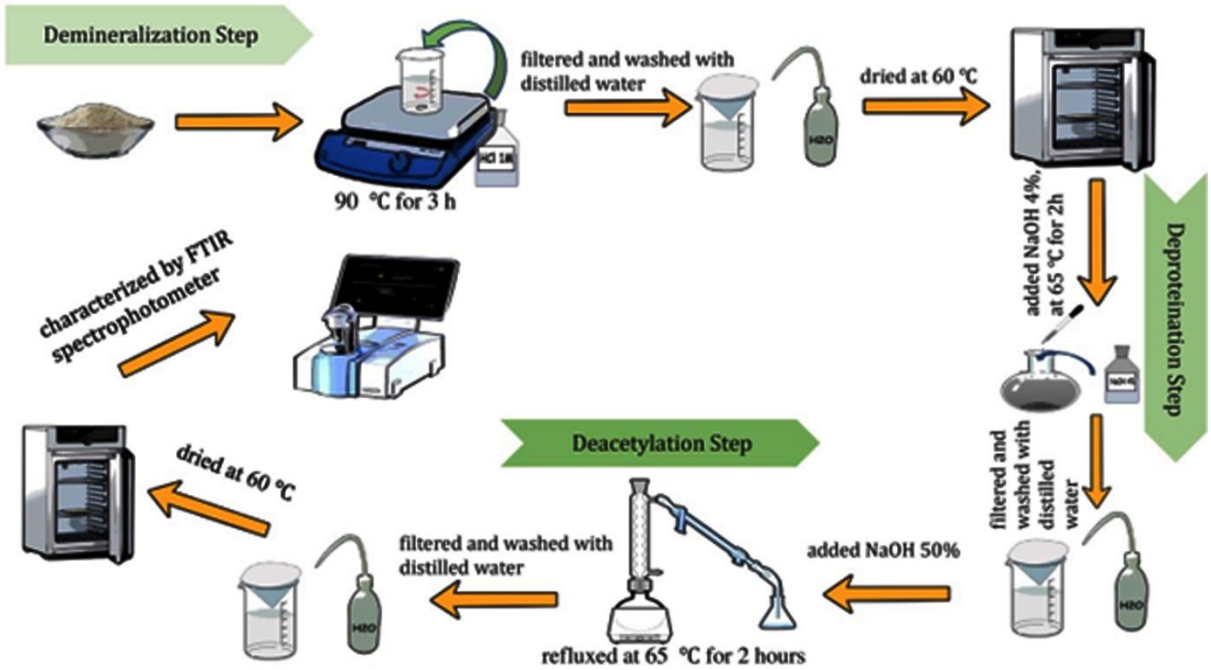

Fig. 2. Schematic illustration of extraction CS from black tiger shrimp shells

2.3 Synthesis CS-NPs

The synthesis of CS-NPs was carried out using the ionic gelation method, CS powder was dissolved in 100 mL of acetic acid 1% to produce CS solution with various concentration (0.1, 0.2, 0.3, 0.4, 0.5 % (wt./v). Then stirred for 1 hour at room temperature. The CS solution was then added with sodium tripolyphosphate (NaTPP) 0.1% (wt./v) and Tween 80 0.1% (v/v) while stirring. The solution was stirred constantly for 2 hours at room temperature, then dried with a spray dryer [26]. The resulting CS-NPs were analyzed using PSA and SEM.

2.4 Antibacterial Activity Test

Samples of CS and CS-NPs were diluted each half from the initial concentration. Then NB medium was added in a volume ratio CS-NPs: NB of 1:1 so that a graded sample dilution would be obtained. After that, each of them was inoculated with 1 mL of the test bacteria, which amounted to $1.5x10^8$ CFU/mL or equivalent to 0.5 Mc Farland. Then incubated at 37 ℃ for 1x24 hours [27]. Tubes showing bacterial growth in the form of turbidity in the media were inoculated on NA media, incubated 1x24 hours, and the number of colonies growing in each concentration series was counted.

3. Results and discussion

3.1 Functional Group and Deacetylation Degree of Chitin, CS, and CS-NPs

Determination of functional groups and DD samples of chitin, CS, and CS-NPs based on the results of the analysis using the FTIR spectrophotometer shown in Fig. 3. Chitin and CS presented some characteristic peaks, at 3400 cm^{-1} is attributed to the -NH_2 and -OH groups stretching vibration and intermolecular hydrogen bonding. In chitin spectra, there are two bands at 1658 cm^{-1} indicating stretching of amide, while stretching C=O indicates hydrogen bonded to N-H groups of the neighbouring intra-sheet chain [28]. The absorption band at 1477 cm^{-1} corresponds to amide II (N-H bending). After the deacetylation step, the 1477 cm^{-1} peak decreased indicating the formation of CS. The similar results were also observed by the previous study, reported that the successful deacetylation

demonstrated by reduction of band at 1655 cm^{-1} and 1400 cm^{-1} assigned to the stretching of C=O in amide bond and CO-NH bending vibration, respectively [29].

The absorption for CS-NPs was indicated by the occurrence of bathochromic shift peaks to about 1700 and 1600 cm^{-1} in the FTIR spectra of CN, which was caused by the interaction between the NH_3^+ group of CS and the phosphate group of TPP. This interaction was also strengthened by a decrease in the intensity of the amide band (1641 cm^{-1}) in CS-NPs compared to chitosan. Furthermore, in CS-NPs a peak appears between 1600 and 1100 cm^{-1} which indicates a characteristic P=O stretching vibration from phosphate groups [30]. It indicates the interaction between positive charge of CS and the negative charge of tripolyphosphate from NaTPP was occurred. Similar results regarding the formation of CS-NPs via TPP crosslinking have been previously reported [18-19]. Polycationic chitosan is formed at an acidic pH with the addition of acetic acid. Meanwhile, polyanionic TPP is formed due to its dissociation in water releasing -OH and $P_3O_{10}^{5-}$ ions which will then react with NH_3^+ from CS [33]. Illustration of the interaction between CS and NaTPP on the formation of CS-NPs by ionic gelation is shown in Fig. 4.

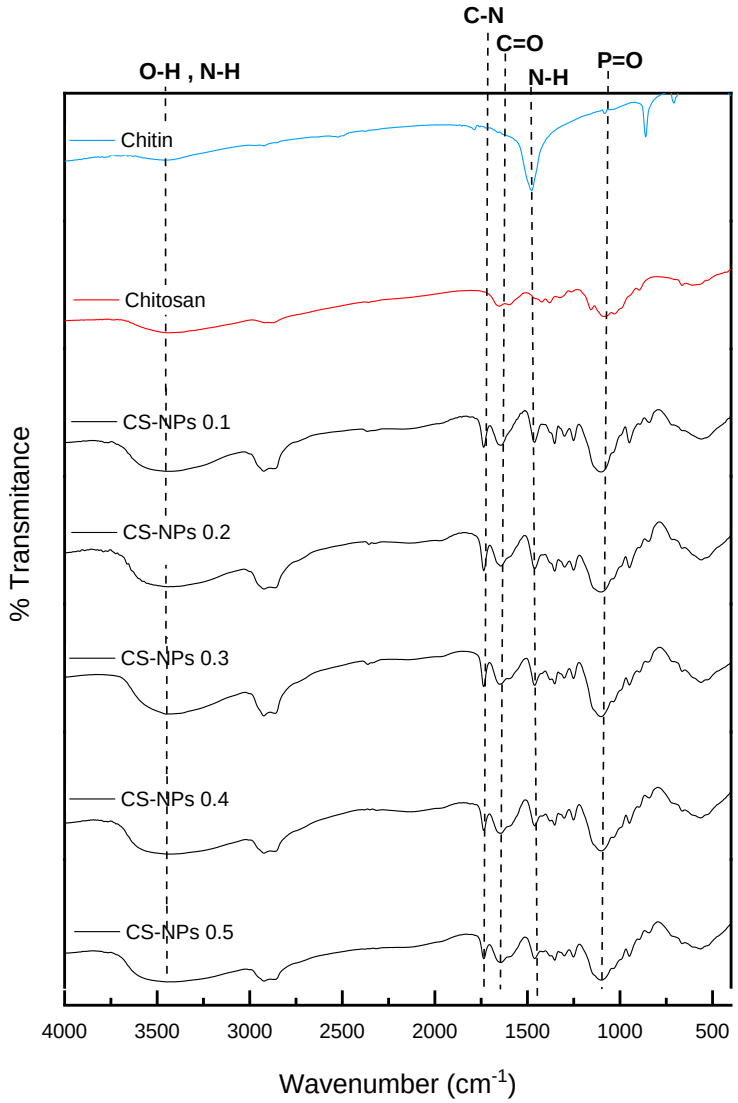

Fig. 3. FTIR spectra of chitin, chitosan, and CS-NPs with various concentration

Based on Fig.3, the DD for each sample can be determined based on equation (1) which is shown in Table 1. An increase in DD from chitin to CS indicates that the deacetylation process has been successfully carried out. The DD CS and CS-NPs are not significantly different. Similar results from previous studies, Sukmawati et al. reported that the initial concentration of CS and tween 80 did not affect the DD value of CS-NPs [34]. Contradically, the report from Abyadeh et al. mentioned that DD value did not

have a significant effect on the particle size of CS-NPs, the most factor that influencing factors is the initial concentration of CS [30]. The DD value in this study is higher than the CS-NPs synthesized from deep-sea mud shrimp, crab shells, and white shrimp shells of 87%, 88.20%, and 75%, respectively [20]–[22].

Table 1. The DD value, particle size, and PI of chitin, CS, and CS-NPs ([a]correspond from FTIR spectra in Fig. 3 and [b]correspond from Fig.5)

Samples	[a]DD (%)	[b]The Average Particle Size (nm)	[b]PI
Chitin	69.58	-	-
Chitosan	93.81	1219	0.511
CS-NPs 0.1%	92.71	92.89	0.556
CS-NPs 0.2%	90.58	127.0	0.501
CS-NPs 0.3%	90.63	283.1	0.561
CS-NPs 0.4%	92.22	363.1	0.632
CS-NPs 0.5%	92.36	407.0	0.703

3.2 Particle Size of CS and CS-NPs

Determination of the particle size of CS and CS-NPs was carried out using PSA. The measurement results are shown in Fig. 5 and the correspond in Table 1. The average particle size of CS from black tiger shrimp shells waste is 1219 nm and has decreased after being synthesized into nanoparticles. Based on Table 1, it can be seen that the size of CS-NPs increased significantly from 92.89 nm to 407 nm with the increasing of initial concentration of CS from 0.1% to 0.5%. This is due to the agglomeration of CS-NPs when the CS concentration increases. When the concentration of CS is low, the intermolecular interaction forces are weak due to the long distance between the molecules, whereas when the concentration of chitosan is high, the intermolecular interactions between chitosan molecules become stronger due to the short distance between the molecules and tends to agglomerate (this is supported by the polydispersity index data).

The results obtained are agreed with the results of Nguyen et al. which varied the initial concentration of CS from 0.3 to 2.1% and the particle size of CS-NPs of 735.9 to 1441.7 nm [33]. In addition, Handani et al. also reported that the initial concentration of CS greatly affects the size of the CS-NPs produced and would also affect the growth of nanoparticles during storage [35].

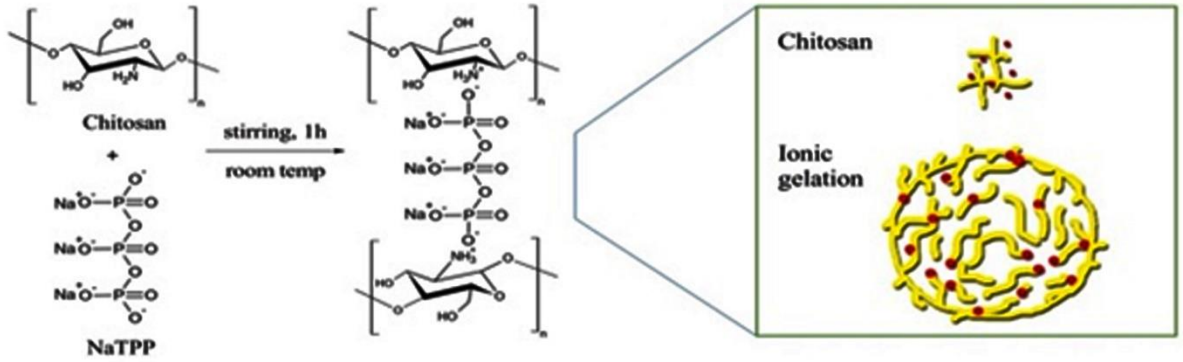

Fig. 4. Electrostatic interaction between chitosan and NaTPP on the formation of CS-NPs. Adapted and modified from Ali et al. [20]

In addition to the average particle size, the results of PSA analysis also show the value of the polydispersity index (PI). The PI value indicates the uniformity of the particle size. Based on Table 1. the distribution of particles is getting more heterogeneous with increasing initial concentration. A PI value below 0.5 indicates a homogeneous particle distribution, while a PI above 0.5 indicates high heterogeneity. Samples of 0.4 and 0.5% CS-NPs had PI values above 0.5 indicating the particles formed aggregates. This is supported by the increasing particle size, as previously discussed. The results obtained are correspond with the results of previous study from Abyadeh et al. [30]. The PI value is higher than previous study (PI 0.232). This is presumably due to this study did not use ultrasound wave [36]. However, the CS-NPS with initial concentration of 0.1% use for the antibacterial activity test.

3.3 Morphology of CS and CS-NPs

The surface morphology of the samples was analysed using SEM as shown in Fig.6. The image showed spherical shape and smooth surface for sample CS and CS-NPs 0.1%. The dendrimer shape for CS-NPS 0.2 and 0.3% and the beads shape for CS-NPS 0.4 and 0.5% [37].

The morphology of the CS sample looks bigger comparing to CS-NPs. The 0.4% and 0.5% CS-NPs

samples showed agglomeration, this was supported by the particle size and PI data and it is in line with the previous study [32]. Something interesting was seen in the morphology of the sample CS-NPs with an initial concentration of 0.2%, showing a uniform morphology. This is presumably because this sample has the lowest DD and PI value (Table 1), indicates the particle distribution was homogenous, furthermore the number of free amino groups is less, which is needed (after protonation) to form a complex with TPP in an acidic solution [28].

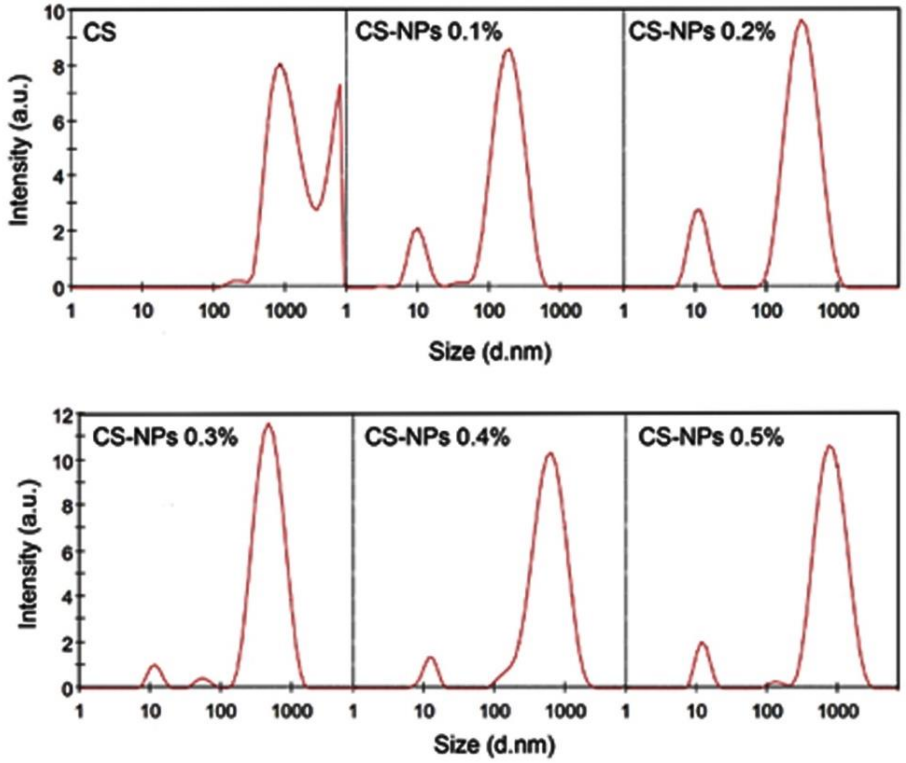

Fig. 5. Particle size distribution of CS and CS-NPs with various initial CS concentration

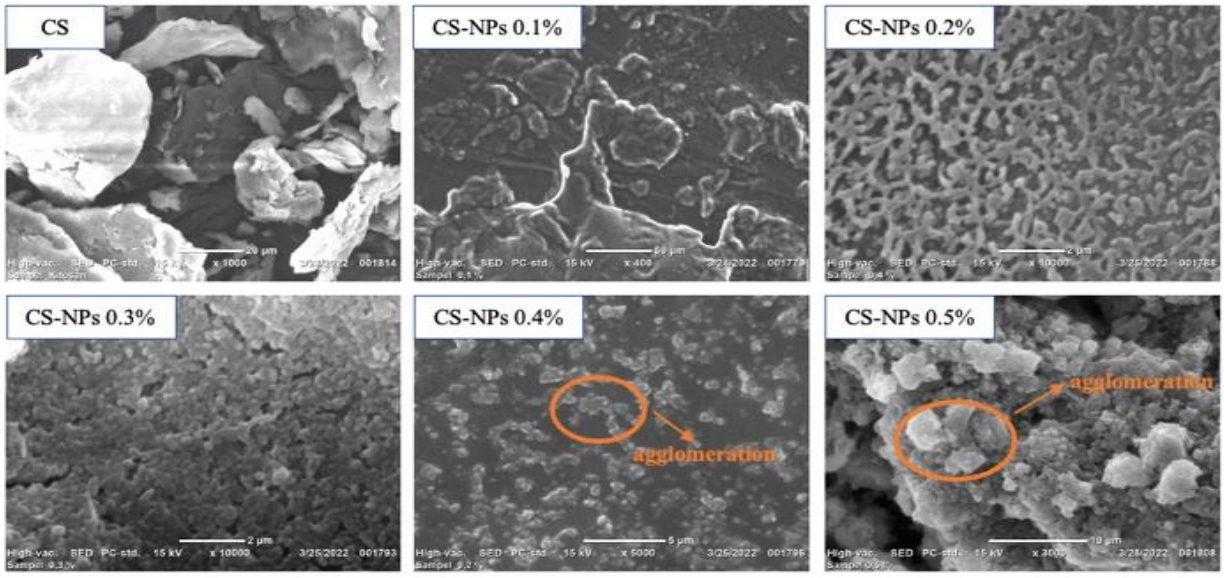

Fig. 6. Surface morphology of CS and CS-NPs analysed using SEM at 15 kV with magnification of 1000x

3.4 Antibacterial Activity of CS and CS-NPs

The results of the MIC test of CS and CS-NPs samples against the growth of *E. coli* and *S. aureus* were carried out using the turbidimetric method as shown in Table 2. The minimum inhibition of bacterial growth with the turbidimetric test occurred at a concentration of 1.250% for both samples because it started to look clear compared to the tube. a small concentration below it is a tube with a concentration of 0.625% to 0.070%.

After the turbidimetric observations were made, it was continued by measuring the absorbance value using a UV-Vis spectrophotometer as shown in Table 3. It shows that at a concentration of 1.250% to 5.000% there has been a decrease in the absorbance value which means that bacterial growth is inhibited and at a concentration of 0.625% the absorbance value before and after incubation increases which means that there is bacterial growth. Thus, the MIC value was at a concentration of 1.250% or twice dilution.

Table 2. MIC test results of CS and CS-NPs samples on the growth of *E.coli* and *S. aureus*

Samples	Concentration (%)	*E. coli*	*S. aureus*
CS	5.000	-	-
	2.500	-	-
	1.250	-	-
	0.625	+	+
	0.320	+	+
	0.160	+	+
	0.070	+	+
CS-NPs	5.000	-	-
	2.500	-	-
	1.250	-	-
	0.625	+	+
	0.320	+	+
	0.160	+	+
	0.070	+	+

Note: The sign (+) indicates that the solution in the tube looks cloudy, which means that bacteria can still grow, while the (-) sign indicates that the solution in the tube looks clear, which means that bacterial growth is inhibited.

The number of colonies growing on agar media was more abundant in CS samples, this indicated that CS-NPs were more active in inhibiting bacterial growth. This is agreed with the results of Yang et al. and Tamara et al. reported that CS-NPs improved the antibacterial activity [28], [38]. Meanwhile, CS and CS-NPs were more active in inhibiting Gram positive (*S. aureus*) than Gram negative (*E. coli*) bacteria as shown in Fig. 7. This is correspond with the results reported before by Goy [39], this is presumably due to the interaction chitosan with cell surface polymers such as teichoic acid of Gram positive bacteria, which is consistent with the fact that binding of CS to the lipopolysaccharide layer of the cell wall of Gram negative bacteria, will not significantly affect susceptibility.

Based on Table 3, CS-NPs have a significant antibacterial activity than CS, this is presumably because of their tiny size and spherical shape. Hosny et al. [8] reported that, generally nanoparticles with a smaller size and spherical shape have a higher surface area so that they are more effective than particles with a larger size and irregular shape in penetrating bacterial cells and causing apoptosis to them. The large surface area facilitated tight absorption to the surface of bacteria leading to disruption of the bacterial membrane and leakage of intracellular compounds and bacterial cell death [38-39].

The lower of CS-NPs concentration, the number of inhibited colonies decreased, as evidenced by the increasing number of colonies observed. This is presumably due to the smaller number of particles that interact permeably with the bacterial cell wall [42]. The ability of the CS-NPs produced against the antibacterial ability of *E. coli* and *S. aureus* is almost similar to the results of previous studies as presented in Table 4.

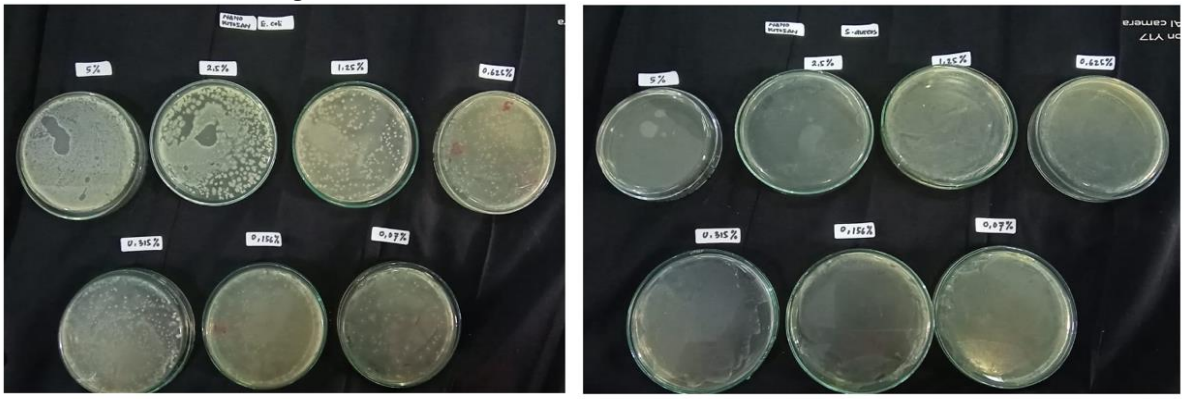

(a) (b)

Fig. 7. Antibacterial activity of CS-NPs against (a) *E. coli* and (b) *S. aureus*

Table 3. The results of the MIC test of CS and CS-NPs samples on the growth of *E.coli* and *S.aureus* using a UV-Vis spectrophotometer and data on the number of colonies on NA media

Samples	Concentration (%)	*E. coli*			*S. aureus*		
		Absorbance Before incubation	Absorbance After incubation	Number of colonies ($x10^7$)	Absorbance Before incubation	Absorbance After incubation	Number of colonies ($x10^7$)
CS	5.000	0.368	0.028	68	1.191	0.554	1
	2.500	0.361	0.329	142	0.704	0.611	8
	1.250	**0.358**	**0.218**	**167**	**0.337**	**0.073**	**9**
	0.625	0.284	0.421	224	0.21	0.022	11
	0.320	0.293	0.423	226	0.158	0.197	13
	0.160	0.281	0.468	246	0.124	0.336	18
	0.070	0.285	0.471	248	0.376	0.681	23
CS-NPs	5.000	0.899	0.378	24	0.611	0.554	1
	2.500	0.768	0.408	87	0.64	0.611	3
	1.250	**0.394**	**0.366**	**153**	**0.341**	**0.073**	**4**
	0.625	0.170	0.195	176	0.088	0.022	5
	0.320	0.015	0.097	232	0.078	0.197	5
	0.160	0.018	0.069	236	0.075	0.336	8
	0.070	0.016	0.512	247	0.068	0.681	10

Table 4. The antibacterial activity of CS-NPs from others feedstock

Feedstock	DD (%)	The Average Particle Size (nm)	PI	MIC		Ref.
				E. coli	*S. aureus*	
Crab shells	85	28.3	<1	1/16	1/8	[43]
Crab shells	90	53.99	1	1/8	1/4	[44]
Shrimp shells	85	394.79	0.45	12.5	6.25	[45]
Shrimp shells	87	120	0.84	40	30	[46]
Black tiger shrimp shells	92	92.89	0.556	1.25	1.25	present

4. Conclusions

The results showed that the degree of deacetylation (DD) of CS-NPs from black tiger shrimp shells waste is more than 90% with the average particle size of CS-NPs being 92.89 nm to 407 nm, increased with increasing initial concentration of CS, which is evidenced by the results of SEM analysis which shows the occurrence of agglomeration. Furthermore, the surface area of CS-NPs showed a spherical shape and smooth surface. Antibacterial activity test showed that CS-NPs have a significant antibacterial activity than CS because of their tiny size and spherical shape. CS-NPs were more active in inhibiting Gram-positive (*S. aureus*) bacteria than Gram-negative (*E. coli*). Therefore, CS-NPs from black tiger shrimp shells waste can be developed for use in other bio-applications in the future.

5. Conflicts of interest

The authors declare that there are no conflicts of interest

6. Acknowledgements

The researcher would like to thank the Biochemistry Laboratory of Hasanuddin University and Research Laboratory of Universitas Negeri Makassar that have supported and assisted in conducting the research.

7. References

[1] J.L. Tucker, The hidden power and competitive advantage of applying green chemistry metrics, Current Opinion Green Sustainable Chemistry, 35(1) (2022), 100606.

[2] S.E. Putri, N. Herawati, A. Fudhail, D.E.Pratiwi, S.S.Desa, A.Surleva, Biosynthesis of Copper Nanoparticles Using Hylocereus costaricensis Peel Extract and their Photocatalytic Properties Biosynthesis of Copper Nanoparticles Using Hylocereus costaricensis Peel Extract and their Photocatalytic Properties, Karbala International Journal Modern Science, 9(2) (2023) 289–306.

[3] A.M. Omer, R. Dey, A.S. Eltaweil, E.M. Abd El-Monaem, and Z. M. Ziora, Insights into recent

advances of chitosan-based adsorbents for sustainable removal of heavy metals and anions, Arabian Journal Chemistry, 15(2) (2022) 103543.

[4] W. Liu, J. Xie, L. Li, Properties of phenolic acid-chitosan composite films and preservative effect on Penaeus vannamei, Journal Molecular Structure, 1239(1) (2021) 130531.

[5] S. Chen, Z. Zhang, X. Wei, Z. Sui, J. Geng, Antibacterial and antioxidant water-degradable food packaging chitosan film prepared from American cockroach, Food Bioscience, 49(2) (2022) 101893.

[6] Y. Cao, S. Alamri, A. A. Rajhi, A. E. Anqi, and A. D. Khalaji, New chitosan Schiff base and its nanocomposite: Removal of methyl green from aqueous solution and its antibacterial activities, International Journal Biology Macromolecule, 192 (2021) 1–6.

[7] B. Tian, Y. Liu, and J. Liu, Chitosan-based nanoscale and non-nanoscale delivery systems for anticancer drugs: A review, European Polymer Journal, 154 (2021) 110533.

[8] M. Hosny, M. Fawzy, E. El-Fakhrany, A. Omer, E. El-Monaem, R. Khalifa, and A. Eltaweil, Biogenic synthesis, characterization, antimicrobial, antioxidant, antidiabetic, and catalytic applications of platinum nanoparticles synthesized from Polygonum salicifolium leaves, Journal Environmental Chemical Engineering, 10(1) (2022) 106806.

[9] S. Chatterjee, A.K. Guha, and B.P. Chatterjee, Evaluation of quantity and quality of chitosan produce from Rhizopus oryzae by utilizing food product processing waste whey and molasses, Journal Environmental Management, 251 (2019) 109565.

[10] M.I. Hidayat, M. Adlim, I. Maulana, S. Suhartono, Z. Hayati, and N.H.H.A. Bakar, Green synthesis of chitosan-stabilized silver-colloidal nanoparticles immobilized on white-silica-gel beads and the antibacterial activities in a simulated-air-filter, Arabian Journal Chemistry, 15(2) (2022) 103596.

[11] K. Li, G. Guan, J. Zhu, H. Wu, and Q. Sun, Antibacterial activity and mechanism of a laccase-catalyzed chitosan–gallic acid derivative against Escherichia coli and Staphylococcus aureus, Elsevier B.V., 96 (2019) 6879.

[12] M.S. Benhabiles, R. Salah, H. Lounici, N. Drouiche, M. F. A. Goosen, and N. Mameri, Antibacterial activity of chitin, chitosan and its oligomers prepared from shrimp shell waste, Food Hydrocolloids, 29(1) (2012) 48–56.

[13] A. Aranda-Martinez, F. Lopez-Moya, and L. V. Lopez-Llorca, Cell wall composition plays a key role on sensitivity of filamentous fungi to chitosan, Journal Basic Microbiology, 56(10) (2016) 1059–1070.

[14] C. Moon, D.J. Seo, Y.S. Song, and W.J. Jung, Antibacterial activity of various chitosan forms against Xanthomonas axonopodis pv. glycines, Elsevier B.V, 156 (2020)..

[15] A.M.L. Kusnadi, Purgiyanti, A.C. Kumoro, The antioxidant and antibacterial activity of chitosan extract from white shrimp shell (Penaueus indicus) in the water nortyh of Brebes, Indonesia, Biodiversity, 23(3) (2022) 1267–1272.

[16] M. Chandrasekaran, K.D. Kim, and S.C. Chun, Antibacterial activity of chitosan nanoparticles: A review, Processes, 8(9) (2020), 1–21.

[17] A.S. Kritchenkov, M.N. Kurasova, A.A. Godzishevskaya, E.S. Mitrofanova, High antibacterial activity and low toxicity of pyridoxal derivatives of chitosan and their nanoparticles, Mendeleev Communication, 31(4) (2021) 504–506.

[18] D. MubarakAli, F.L. Oscar, V. Gopinath, N.S. Alharbi, S.A. Alharbi, and N. Thajuddin, An inhibitory action of chitosan nanoparticles against pathogenic bacteria and fungi and their potential applications as biocompatible antioxidants, Microbiology Pathogenesis, 114(2) (2018) 323–327.

[19] T. Di Nardo, C. Hadad, A. Nguyen Van Nhien, and A. Moores, Synthesis of high molecular weight chitosan from chitin by mechanochemistry and aging, Green Chemistry, 21(12) (2019) 3276–3285.

[20] E. Rochima, S.Y. Azhary, R.I. Pratama, C. Panatarani, and I.M. Joni, Preparation and Characterization of Nano Chitosan from Crab Shell Waste by Beads-milling Method, IOP Conference Series Material Science Engineering, 193(1) (2017).

[21] M.E.A. Ali, M.M.S. Aboelfadl, A.M. Selim, H.F. Khalil, and G.M. Elkady, Chitosan nanoparticles extracted from shrimp shells, application for removal of Fe(II) and Mn(II) from aqueous phases, Separation Science Technology, 53(18) (2018) 2870–2881.

[22] M.K. Rasweefali, S. Sabu, K.V. Sunooj, A. Sasidharan, and K.A.M. Xavier, Consequences of chemical deacetylation on physicochemical, structural and functional characteristics of chitosan extracted from deep-sea mud shrimp, Carbohydrate Polymer Technology Application, 2(12) (2021) 100032.

[23] B. Arasukumar, G. Prabakaran, B. Gunalan, and M. Moovendhan, Chemical composition, structural features, surface morphology and bioactivities of chitosan derivatives from lobster (Thenus unimaculatus) shells, International

Journal Biological Macromolecule, 1359(4) (2019) 1237–1245.
[24] C.T. Doan, T.N. Tran, V.B. Nguyen, T.P.K. Vo, A.D. Nguyen, and S.L. Wang, Chitin extraction from shrimp waste by liquid fermentation using an alkaline protease-producing strain, Brevibacillus parabrevis, International Journal Biology Macromolecule, 131(2) (2019) 706–715.
[25] L.M.H. Nadia, P. Suptijah, and B. Ibrahim, Production and Characterization Chitosan Nano from Black Tiger Shrimpwith Ionic Gelation Methods, Journal of King Saud University, 17(2) (2018) 119–126.
[26] T. Wu C. Wu, S. Fu, L. Wang, C. Yuan, Integration of lysozyme into chitosan nanoparticles for improving antibacterial activity, Carbohydrate Polymer, 155 (2019) 192–200.
[27] M.J. Fatemi, S. Garahgheshlagh, T. Ghadimi, Investigating the Impact of Collagen-Chitosan Derived from Scomberomorus Guttatus and Shrimp Skin on Second-Degree Burn in Rats Model, Regenerative Therapy, 18(2) (2021) 12–20.
[28] H.C. Yang and M.H. Hon, The effect of the degree of deacetylation of chitosan nanoparticles and its characterization and encapsulation efficiency on drug delivery, Polymer-Plastic Technology Engineering, 49(12) (2010) 1292–1296.
[29] H. Aldila, Asmar, V.A. Fabiani, D.Y. Dalimunthe, and R. Irwanto, The effect of deproteinization temperature and NaOH concentration on deacetylation step in optimizing extraction of chitosan from shrimp shells waste, IOP Conference Series Earth Environmental Science, 599 (2020).
[30] M. Abyadeh, A.A. Karimi Zarchi, M.A. Faramarzi, and A. Amani, Evaluation of factors affecting size and size distribution of chitosan-electrosprayed nanoparticles, Avicenna Journal Medical Biotechnology, 9(3) (2017) 126–132.
[31] H.M. Ibrahim, A. E.H.A., and S. H.A., Haloperidol-loaded chitosan nanocomposites improve liver and kidney functions and lipid profile of male rats, Research Journal Pharmaceutical, Biological and Chemical Science, 8(3) (2017) 1135–1145.
[32] R.A. Shapi'i, S.H. Othman, M.N. Naim, and R. K. Basha, Effect of initial concentration of chitosan on the particle size of chitosan nanoparticle, International Journal Nanotechnology, 16(11-12) (2019) 680–691.
[33] T.V. Nguyen, T.T.H. Nguyen, S.L. Wang, T.P.K. Vo, and A.D. Nguyen, Preparation of chitosan nanoparticles by TPP ionic gelation combined with spray drying, and the antibacterial activity of chitosan nanoparticles and a chitosan nanoparticle–amoxicillin complex, Research on Chemical Intermediates, 43(6) (2017) 3527–3537.
[34] A. Sukmawati, W. Utami, R. Yuliani, M. Da'I, and A. Nafarin, Effect of tween 80 on nanoparticle preparation of modified chitosan for targeted delivery of combination doxorubicin and curcumin analogue, IOP Conference Series Material Science Engineering, 311(1) (2018).
[35] W.R. Handani, W.B. Sediawan, A. Tawfiequrrahman, Wiratni, and Y. Kusumastuti, The effect of temperature and chitosan concentration during storage on the growth of chitosan nanoparticle produced by ionic gelation method, AIP Conference Proceeding, 1840 (2017).
[36] E. Rostami, S. Kashanian, and M. Askari, The effect of ultrasound wave on levothyroxine release from Chitosan nanoparticles, Advanced Materials Research, 829(11) (2014) 284–288.
[37] X. Li A. Radomski, O. Corrigan, Tajber, Platelet compatibility of PLGA, chitosan and PLGA-chitosan nanoparticles, Nanomedicine, 4(7) (2009) 735–746.
[38] F.R. Tamara, C. Lin, F.L. Mi, and Y.C. Ho, Antibacterial effects of chitosan/cationic peptide nanoparticles, Nanomaterials, 8(2) (2018) 1–15.
[39] R.C. Goy, S.T.B. Morais, and O.B.G. Assis, Evaluation of the antimicrobial activity of chitosan and its quaternized derivative on E. coli and S. aureus growth, Revista Brasileira Farmacognosia, 26(1) (2016) 122–127.
[40] F.S. Youssef, G.G. Mohamed, S.H. Ismail, H.Y. Elzorba, A. M. Galal, and H. A. Elbanna, Synthesis, characterization and in vitro antimicrobial activity of florfenicol-chitosan nanocomposite, Egyptian Journal of Chemistry, 64(2) (2021) 941–948.
[41] F. Cava, H. Lam, M.A. de Pedro, and M.K. Waldor, Emerging knowledge of regulatory roles of d-amino acids in bacteria, Cellular Molecular Life Science, 68(5) (2011) 817–831.
[42] A. Ivask A. ElBadway, C. Kaweeteerawat, D. Boren, Toxicity Mechanisms in Escherichia coli Vary for Silver Nanoparticles and Differ from Ionic Silver, ACS Nano, 8(1) (2014) 374–386.
[43] L. Qi, Z. Xu, X. Jiang, C. Hu, and X. Zou, Preparation and antibacterial activity of chitosan nanoparticles, Carbohydrate Research, 339(16) (2014) 2693–2700.
[44] W.L. Du, S.S. Niu, Y.L. Xu, Z.R. Xu, and C.L. Fan, Antibacterial activity of chitosan molecule

tripolyphosphate nanoparticles loaded with various metal ions, Carbohydrate Polymer, 75(3) (2019) 385–389.

[45] A. Sarwar, H. Katas, and N.M. Zin, Antibacterial effects of chitosan–tripolyphosphate nanoparticles: impact of particle size molecular weight, Journal Nanoparticle Research, 16(7) (2018) 2517.

[46] K. Divya, S. Vijayan, T. K. George, and M. S. Jisha, Antimicrobial properties of chitosan nanoparticles: Mode of action and factors affecting activity, Fibers Polymer, 18(2) (2017) 221–230.